Non-Coherent Open-loop MIMO Communications Over Temporally-Correlated Channels

Jorge Cabrejas, Sandra Roger, *Member*, *IEEE*, Daniel Calabuig, *Member*, *IEEE*, Yaser M. M. Fouad, Ramy H. Gohary, *Senior Member*, *IEEE*, Jose F. Monserrat, *Senior Member*, *IEEE*, and Halim Yanikomeroglu, *Senior Member*, *IEEE*

***Abstract*—This paper investigates the use of non-coherent communication techniques for open-loop transmission over temporally-correlated Rayleigh-fading Multiple Input Multiple Output (MIMO) channels. These techniques perform data detection without knowing the instantaneous channel coefficients. Three non-coherent MIMO schemes, namely Differential Unitary Space-Time Modulation (DUSTM), differential Space-Time Block Code (STBC) and Grassmannian signaling, are compared with several state-of-the-art training-based coherent schemes. This paper shows that the non-coherent schemes are meaningful alternatives to training-based communication, specially as the number of transmit antennas increases. In particular, for more than two transmit antennas, non-coherent communication provides a clear advantage in medium to high mobility scenarios.**

***Index Terms*—Non-coherent communications, Grassmannian signaling, DUSTM, differential STBC, MIMO, temporal correlation.**

I. Introduction

The Fourth Generation (4G) cellular standards are based on coherent detection, which requires the knowledge of the channel coefficients at the receiver side. For this purpose, the transmitter sends training data to the receiver in the form of pilot symbols, which spend a portion of the available resources that could have been otherwise allocated for data transmission [1]. Moreover, this drawback becomes more pronounced as the number of transmit antennas increases. This limitation of training-based open-loop communications triggered the increasing research interest in non-coherent MIMO communication techniques, which perform data detection without any knowledge of the channel coefficients at the receiver side, other than the channel statistics. In this direction, several non-coherent schemes have been proposed in the literature for MIMO communications [2]–[8].

Some authors generalized the concept of differential modulation from single-antenna to multiple-antenna systems. In particular, a method called DUSTM was proposed in [3], in which the transmitted signal consists of an $M \times M$ unitary matrix multiplied by an $M \times M$ unitary matrix transmitted during the previous M channel uses. This differential encoding allows the receiver to recover the transmitted signal through the previous received block of M channel uses. Other prominent schemes based on the same principle are the differential STBC [4], which is based on Alamouti coding, and the Cayley differential codes [5], which make use of the Cayley transform to generate a meaningful set of unitary matrices for differential transmission and reception.

Apart from differential modulation, there exist other non-coherent schemes whose optimal input signals are designed taking into account that, in a *block-fading* channel and at high Signal to Noise Ratio (SNR), the columns of the received signal are a linear combination of the columns of transmitted signal. Taking into account that the channel coefficients of a block-fading channel remain constant over blocks of several channel uses, after the transmission through these channels, it can be shown that the subspace spanned by the columns of the transmitted and received matrices is the same. Thus, these observations suggest that, at high SNR, the transmitter should map the information to distant subspaces in order to minimize the error probability. Under the above assumptions, the authors in [2] showed that the optimal capacity-achieving input signals are unitary matrices isotropically distributed on the compact Grassmann manifold. Signal constellations that mimic the high-SNR capacity-achieving isotropic distribution can be found in [6] and references therein. This non-coherent scheme is often referred to as Grassmannian signaling.

In practical scenarios, however, the block-fading channel assumption is often unrealistic due to the relative speed between transmitter and receiver. Although there is an extensive number of contributions on the performance analysis of coherent schemes in temporally-correlated channels, the impact of the speed on the performance of non-coherent schemes based on differential modulation and Grassmannian signaling is still an open issue. In fact, the non-coherent capacity over these channels is still unknown even for the Single Input Single Output (SISO) case. In [9], the performance of the Differential Space-Time Modulation (DSTM) in frequency-selective temporally-correlated channels was evaluated, considering two transmit antennas but only one receive antenna. This work compared the performances of DSTM and Alamouti coding [10] and showed an unnecessarily pessimistic result for the coherent scheme.

In this paper, we consider a temporally-correlated MIMO channel to compare various non-coherent techniques with several benchmark training-based coherent schemes designed for the same number of transmit and receive antennas. In particular, we analyze the performance of three different non-

Jorge Cabrejas, Sandra Roger, Daniel Calabuig and Jose F. Monserrat are with the Institute of Telecommunications and Multimedia Applications, Universitat Politècnica de València (UPV), Valencia, 46022 Spain, e-mail: {jorcabpe, sanrova, dacaso, jomondel}@iteam.upv.es.

Yaser M. M. Fouad, Ramy H. Gohary and Halim Yanikomeroglu are with the Department of Systems and Computer Engineering, Carleton University, Ottawa, ON, Canada, e-mail: {yfouad, gohary, halim}@sce.carleton.ca.

coherent communication schemes, two of them based on differential communication (the DUSTM in [3] and the differential STBC in [4]) and a third one based on Grassmannian signaling [2]. The selected baselines for two transmit antennas are the Alamouti [10] and Golden codes [11] and, for four transmit antennas, the rate-$3/4$ STBC in [12] and the Quasi-Orthogonal Space-Time Block Code (QOSTBC) in [13].

The rest of the paper is organized as follows. Section II describes the system model. In Section III, the set of training-based coherent schemes to be used as baselines for comparison are presented. Section IV and Section V, elaborate on the two types of non-coherent schemes analyzed in this paper. In Section VI, the specific coherent and non-coherent configurations that will be evaluated are presented, together with the simulation results and discussions. Finally, Section VII summarizes the results of this work and concludes the paper.

II. System model

We consider a single-user link with M transmit antennas and N receive antennas ($M \times N$ MIMO system). The transmitter uses space-time modulation to send information blocks of K bits over T channel uses and M transmit antennas. The transmission rate in bits per channel use (bpcu) is $R = K/T$. Each block consists of a $T \times M$ complex matrix

$$\mathbf{X} = [\mathbf{x}_1, \mathbf{x}_2, \ldots, \mathbf{x}_t, \ldots, \mathbf{x}_T]^\intercal,$$

where $\mathbf{x}_t \in \mathbb{C}^{M\times 1}$, $t \in \{1, \ldots, T\}$, is the signal transmitted by the M antennas at channel use t, and the superscript $\intercal$ stands for matrix transposition operation. After T channel uses, the receiver processes the $T \times N$ matrix $\mathbf{Y} = [\mathbf{y}_1, \mathbf{y}_2, \ldots, \mathbf{y}_t, \ldots, \mathbf{y}_T]^\intercal$, where

$$\mathbf{y}_t^\intercal = \mathbf{x}_t^\intercal \mathbf{H}_t + \sqrt{\frac{M}{\rho T}}\mathbf{z}_t^\intercal \tag{1}$$

is the complex vector received at channel use t, $\mathbf{z}_t \in \mathbb{C}^{N\times 1}$ is the complex-valued Additive White Gaussian Noise (AWGN) vector at channel use t with zero-mean and unit-variance components, i.e. $\mathbb{E}[\mathbf{z}_t\mathbf{z}_t^{\mathrm{H}}] = \mathbf{I}_N$, ρ is the SNR and $\mathbf{H}_t \in \mathbb{C}^{M\times N}$ is the channel matrix between the transmit and receive antennas at channel use t.

We assume that the channel is temporally-correlated through a sum-of-sinusoids statistical model, which is an improved version of the original Jakes' model [14]. In this model, correlation between two samples separated by T_s seconds is $J_0(2\pi f_d T_s)$. Here, J_0 is the zeroth-order Bessel function of the first kind, $f_d = v f_c/c$ is the Doppler frequency, v is the relative speed between the transmitter and the receiver, f_c is the carrier frequency of the signal and the constant $c = 3 \cdot 10^8$ m/s is the speed of light.

In this work, two different types of detectors are considered at the receiver side, namely the coherent detector, which has availability of the channel coefficients for the detection, and the non-coherent one, which works without any knowledge of the channel. Figures 1 (a) and (b) show the block diagram of the transmitter and receiver of the coherent and non-coherent schemes, respectively. It can be observed that the coherent setup includes a channel estimation stage to acquire the channel coefficients, as it will be next elaborated. Particularizations of these two MIMO schemes are deeply analyzed in Section III, Section IV and Section V.

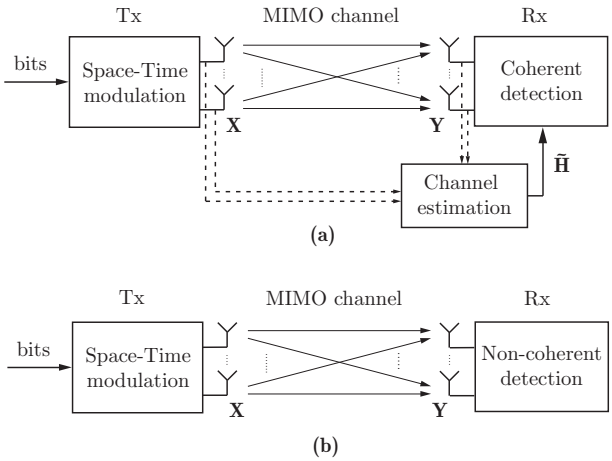

Fig. 1: Block diagram of the evaluated MIMO system. (a) With coherent detection, (b) with non-coherent detection.

III. Coherent training-based schemes

This section describes the transmitter and receiver of the coherent schemes analyzed in this paper, namely the Alamouti code, rate-3/4 STBC, QOSTBC, and Golden code.

A. Encoding

The well-known coding scheme proposed by Alamouti is the simplest full-diversity Orthogonal Space-Time Block Code (OSTBC) for the two transmit antenna case. In this scheme, $T = M = 2$ and the 2×2 transmission matrix is structured as follows [10]:

$$\mathbf{X} = \begin{bmatrix} s_1 & s_2 \\ -s_2^* & s_1^* \end{bmatrix}, \tag{2}$$

where the symbols s_i, $i = 1, 2$, are taken from a Quadrature Amplitude Modulation (QAM) constellation Ω of size $|\Omega|$ and hence carry $\log_2(|\Omega|)$ code bits each.

We will also include the Golden code for two antennas with $T = 2$, which is a full-rate and full-rank STBC with the following code matrix [11]:

$$\mathbf{X} = \frac{1}{\sqrt{5}}\begin{bmatrix} \alpha(s_1 + s_2\theta) & \alpha(s_3 + s_4\theta) \\ i\gamma\left(s_3 + s_4\bar{\theta}\right) & \gamma(s_1 + s_2\bar{\theta}) \end{bmatrix},$$

where $\theta = \frac{1+\sqrt{5}}{2}$ is the Golden number, $\gamma = 1 + i\theta$ with $i = \sqrt{-1}$, $\bar{\theta} = 1 - \theta$ and $\alpha = 1 + i\bar{\theta}$.

For the $M = 4$ case, we will include the performance of a STBC of rate $3/4$ [15] within the comparisons, which is transmitted using $T = 4$ channel uses. Its code matrix, defined in [12], is

$$\mathbf{X} = \begin{bmatrix} s_1 & 0 & -s_2^* & s_3^* \\ 0 & s_1 & -s_3 & -s_2 \\ s_2 & s_3^* & s_1^* & 0 \\ -s_3 & s_2^* & 0 & s_1^* \end{bmatrix}^\intercal.$$

Another alternative that will be evaluated is the QOSTBC [13], which needs $T = 4$ channel uses for its transmission and has the following code matrix

$$\mathbf{X} = \begin{bmatrix} s_1 & -s_2^* & -s_3^* & s_4 \\ s_2 & s_1^* & -s_4^* & -s_3 \\ s_3 & -s_4^* & s_1^* & -s_2 \\ s_4 & s_3^* & s_2^* & s_1 \end{bmatrix}^{\mathsf{T}}.$$

B. Decoding

Coherent codes will be decoded using Maximum Likelihood (ML) decoding. The ML decoding metric to be minimized over all possible values of codewords $\mathbf{X}$ for the Alamouti, rate-3/4 STBC, QOSTBC and Golden codes is given by

$$\hat{\mathbf{X}} = \arg\min_{\mathbf{X}} \|\mathbf{Y} - \mathbf{X}\widetilde{\mathbf{H}}\|^2, \tag{3}$$

where $\widetilde{\mathbf{H}}$ is an estimate of the channel matrix. Here we assume a training-based scheme where an $M \times M$ matrix $\mathbf{P}$ containing training symbols is used to acquire the channel coefficients at the receiver side via Minimum Mean Square Error (MMSE) channel estimation [1], [16], that is,

$$\widetilde{\mathbf{H}} = \sqrt{\frac{M}{\rho}} \left(\frac{\rho}{M} \mathbf{I}_M + \mathbf{P}^{\mathrm{H}}\mathbf{P} \right)^{-1} \mathbf{P}^{\mathrm{H}}\mathbf{Y}_{\mathrm{P}},$$

where ρ and $\mathbf{P}$ are known a priori by the receiver and $\mathbf{Y}_{\mathrm{P}}$ denotes the signal matrix received after the transmission of pilots.

IV. Non-Coherent differential schemes

This section describes the transmitter and receiver of two non-coherent differential schemes, namely DUSTM and differential STBC. These schemes are extensions of the Differential Phase Shift Keying (DPSK) modulation to support MIMO communications [3]. As in every differentially-encoded constellation, each transmitted signal in this scheme is a reference for the following one.

Non-coherent differential schemes are intended for slow-fading channels, where the channel can be assumed approximately constant during any $2M$ consecutive channel uses. However, for fast-fading channels, this assumption is not valid any longer and both DUSTM and differential STBC deteriorate as the normalized Doppler frequency increases.

A. DUSTM

We will consider here the DUSTM scheme proposed in [3] for two and four transmit antennas.

1) Encoding: The codebook of symbols consists of a set of $M \times M$ unitary matrices, i.e., $T = M$ in this coding scheme. The signal matrix to be transmitted is differentially encoded from the matrix transmitted in the previous block of M channel uses, denoted by $\bar{\mathbf{X}}$, as

$$\mathbf{X} = \mathbf{V}_l \bar{\mathbf{X}}. \tag{4}$$

Here, $\mathbf{V}_l$, $l = \{0, 1, \ldots, L-1\}$, belongs to a codebook of $L = 2^{RM}$ $M \times M$ unitary diagonal matrices. As introduced in [3], the performance of this codebook is significantly degraded for $R > 2$, a result that will be later verified by simulations in Section VI-B. Note that, to initialize the communication, the first $\bar{\mathbf{X}}$ is supposed to be a training matrix equal to an $M \times M$ identity matrix.

2) Decoding: With the approximation that the channel is constant during $2M$ channel uses and equal to $\mathbf{H}$, the received signals in two consecutive blocks are

$$\bar{\mathbf{Y}} = \bar{\mathbf{X}}\mathbf{H} + \sqrt{\frac{M}{\rho T}}\bar{\mathbf{Z}}, \tag{5}$$

$$\mathbf{Y} = \mathbf{X}\mathbf{H} + \sqrt{\frac{M}{\rho T}}\mathbf{Z}, \tag{6}$$

where $\mathbf{Z} = [\mathbf{z}_1, \mathbf{z}_2, \ldots, \mathbf{z}_t, \ldots, \mathbf{z}_T]^{\mathsf{T}}$ is the $T \times N$ noise matrix and $\bar{\mathbf{Z}}$ denotes the noise matrix of the previous transmission.

Including (4) into (6) and combining with (5), we obtain

$$\mathbf{Y} = \mathbf{V}_l \bar{\mathbf{Y}} + \sqrt{\frac{M}{\rho T}}(\mathbf{Z} - \mathbf{V}_l \bar{\mathbf{Z}}), \tag{7}$$

which is the fundamental differential receiver equation. Note that although, here, the desired signal is corrupted by noise with twice the variance, the channel matrix is no longer necessary for the detection stage. This results in the well-known 3 dB performance loss in effective SNR when the channel is unknown in comparison when it is known. The ML detection rule is directly

$$\hat{\mathbf{V}} = \arg\min_{l} \|\mathbf{Y} - \mathbf{V}_l \bar{\mathbf{Y}}\|^2, \tag{8}$$

where the notation $\hat{\mathbf{V}}$ is used for the detected codeword. Note that, if the channel is not constant during 2M channel uses, Equation (7) does not hold and the detection rule in (8) involves some performance degradation.

B. Differential STBC

Another alternative considered in our study is the differential STBC scheme proposed in [4] for two transmit antennas, which combines Alamouti coding with the concept of differential transmission and reception. We further assume two receiver antennas, in contrast to the single receive antenna case shown in [4] and [17].

1) Encoding: The original scheme considers symbols drawn from a Phase-Shift Keying (PSK) constellation Ω of size $|\Omega|$, the symbols of which carry $K = \log_2(|\Omega|)$ code bits each. A variant of the scheme to support QAM constellations was later proposed in [17].

When the communication starts, the transmitter selects two arbitrary symbols s_1 and s_2 and generates a first matrix to be transmitted, $\bar{\mathbf{X}}$, as the Alamouti encoding of s_1 and s_2 (see Equation (2)). Note that these two symbols are unknown to the receiver and carry no information. Next, the transmitter picks a set of $2K$ information bits and generates two coefficients, A and B, where A is constructed based on the first K bits to be transmitted and B is constructed based on the last K bits, as further elaborated in [4]. Using these two coefficients and the matrix transmitted in the previous two channel uses, the

next symbols to be transmitted, s_3 and s_4, are computed as follows:

$$\begin{bmatrix} s_3 \\ s_4 \end{bmatrix} = \bar{\mathbf{X}}^{\intercal} \begin{bmatrix} A \\ B \end{bmatrix}.$$

Finally, the Alamouti encoding of symbols s_3 and s_4 is transmitted to the channel:

$$\mathbf{X} = \begin{bmatrix} s_3 & s_4 \\ -s_4^* & s_3^* \end{bmatrix}.$$

The procedure is repeated until no further information data is available, always constructing the current symbols based on the symbols transmitted in the previous two channel uses.

2) Decoding: As in the DUSTM case, the channel is considered approximately constant during $2M$, i.e. 4, channel uses and equal to $\mathbf{H}$. This leads to the received signals in two consecutive blocks obtained in Equations (5) and (6). The differential decoder then computes:

$$r = \text{vec}(\mathbf{Y})^{\text{H}}\text{vec}(\bar{\mathbf{Y}}) = \alpha A + z, \tag{9}$$

where α is related to the channel coefficients between the i-th transmitter antenna and the k-th receiver antenna, $h_{i,k}$, for $i = 1, 2$ and $k = 1, 2$, as $\alpha = \sum_{ik} |h_{i,k}|^2$. The operation $\text{vec}(\mathbf{Y})$ denotes the $NT \times 1$ vector obtained by stacking columns of $\mathbf{Y}$ and z is a noise term with the same statistical properties as $\bar{\mathbf{Z}}$ and $\mathbf{Z}$. From (9), the receiver can directly estimate the A coefficient doing a closest-point search. A similar procedure is followed to estimate coefficient B. Please refer to [4] and [17] for further details. Once A and B are estimated, an inverse mapping is applied to recover the $2K$ transmitted bits.

V. Non-coherent scheme based on Grassmannian codes

A. Encoding

The idea behind this encoding scheme is based on the observation that, in a block-fading channel and at high SNR, when the $T \times M$ input signal matrix $\mathbf{X}$ is passed through a complex MIMO channel, the columns of the received matrix $\mathbf{Y}$ are linear combinations of the columns of $\mathbf{X}$. Due to this, the subspaces spanned by the columns of $\mathbf{X}$ and $\mathbf{Y}$ are the same. Therefore, the transmitter has to only map the transmitted matrices to distant subspaces, represented by the codewords that compose the Grassmannian constellation Ψ. For instance, several design methods for Grasmannian constellations can be found in [6], where the design criterion is based on selecting distant subspaces in order to minimize the error probability. Figure 2 shows an exemplary Grassmannian constellation composed of four different directions in a plane, which can be represented by four 2×1 matrices, i.e. four one-dimensional subspaces in a two-dimensional space.

B. Decoding

The particular subspace basis rotation is not detectable by a receiver without channel knowledge. However, the M-dimensional linear subspace spanned by this basis can be detected by using a Generalized Likelihood Receiver Test (GLRT) [18]. The GLRT criterion projects the received signal on the different subspaces that compose the Grassmannian constellation. Then, it calculates the energies of all the projections and selects the projection that maximizes the energy as follows

$$\hat{\mathbf{X}} = \arg\max_{\mathbf{S}\in\Psi} \text{Tr}(\mathbf{Y}^{\text{H}}\mathbf{S}\mathbf{S}^{\text{H}}\mathbf{Y}), \tag{10}$$

where Ψ is the set of matrices in the Grassmannian constellation. From the perspective of average symbol error probability minimization, in general, the GLRT provides a suboptimal result compared to the ML criterion. However, for the case of unitary constellations assumed in this work, GLRT offers ML detection performance [18].

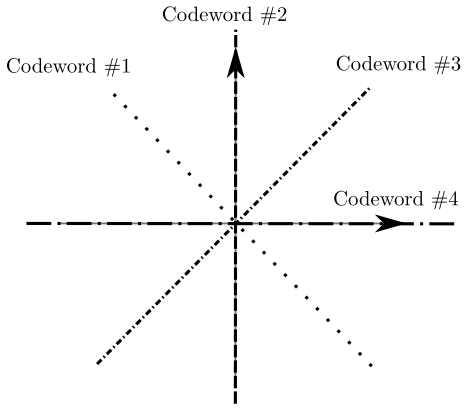

Fig. 2: Exemplary Grassmannian codebook for $M = 1$ antenna and $T = 2$ channel use: 4 different directions in a plane.

An exemplary procedure for transmission and detection of a Grassmannian constellation during T channel uses is described next. Figure 3 shows the block diagram of the associated non-coherent transceiver which uses $M = 1$ antenna, $T = 2$ channel uses and the Grassmannian constellation in Figure 2. First of all, the information bits to be transmitted are mapped to Codeword #3 through the matrix $\mathbf{X}$ (see Figure 2). After the codeword is transmitted, its underlying basis (the dark arrow in the subspace) is transformed by the channel, but it remains in the same subspace. Note that, in this example, the channel h is the same for the two channel uses. Although the non-coherent receiver cannot detect the particular transformation caused by the channel, at high SNR, that is, with negligible effect of the noise vector, it can indeed detect the subspace spanned by this basis. Therefore, the transmitted information can be recovered without any knowledge of the channel at the receiver.

VI. Simulation results

In this section, we present the specific coherent and non-coherent configurations that will be evaluated, together with the simulation results and discussions.

A. Configurations to be evaluated

The aim of this paper is to compare the performance of coherent and non-coherent open-loop communication schemes under realistic assumptions of channel variability caused by mobility. In order to evaluate the behavior of the different schemes with respect to the transmission rate, we consider two exemplary values of this rate for a 2×2 system, particularly

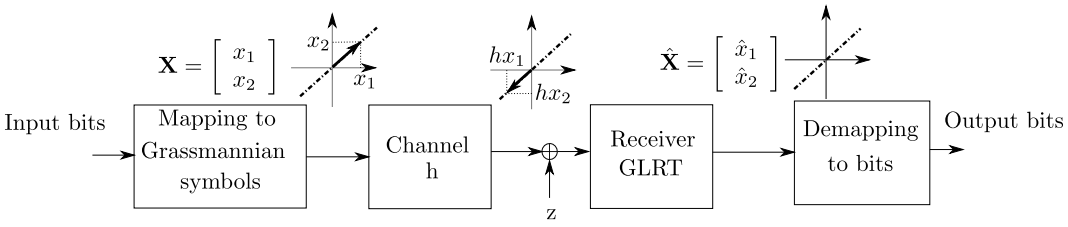

Fig. 3: Block diagram of a non-coherent transceiver with $M = 1$ antenna and $T = 2$ channel uses.

$R = 2$ bpcu and $R = 3$ bpcu, at an SNR value of 25 dB. Moreover, to see the effect of increasing the number of antennas, we will also evaluate a 4×4 system for the $R = 2$ bpcu case and the same SNR value. The simulated coherent schemes for two transmit antennas and two channel uses are the well-known Alamouti and the Golden code schemes [10] [11]. For the $M = 4$ case, we include the performance of a STBC of rate $3/4$ within the comparisons, which is transmitted using 4 channel uses [15]. Another alternative that will be evaluated is the use of a QOSTBC [13], which also needs 4 channel uses for its transmission. For all schemes, a ML receiver will be used. Only coherent schemes use a MMSE channel estimator [1], [16].

Figure 4 shows the transmission configurations of coherent and non-coherent schemes analyzed in this paper. Unlike the coherent schemes, Grassmannian signalling does not need any prior transmission of pilots and its design rule assumes a block-fading channel of duration T channel uses. Although the temporally-correlated channel does not match this feature, we will evaluate designs assuming $T = 4$, $T = 6$ and $T = 8$ for the 2×2 case, and, $T = 8$ and $T = 12$ for the 4×4 case to see the degradation of assuming large block lengths under temporal correlation. Recall that, in the case of DUSTM and differential STBC, there is a unique transmission of a $M \times M$ pilot matrix at the beginning of the communication, whose overhead can be disregarded assuming a high number of transmission blocks. On the other hand, coherent schemes require the transmission of a certain amount of pilots for channel estimation [16]. In order to estimate correctly the channel, at least one pilot symbol per antenna is needed every channel coherence time (T_c). In this work, we followed the approach of cellular standards such as Long Term Evolution (LTE), where the percentage of training symbols is obtained for a maximum Doppler frequency and it is fixed for all the possible values of this parameter. Considering a reference maximum speed of 250 km/h (high speed trains or motorways), and assuming the symbol period of the LTE standard, that is $T_s = 66.67\ \mu s$, and a carrier frequency $f = 2$ GHz, this leads to a normalized Doppler frequency of $f_d T_s = 0.03$ and to a coherence time [19]:

$$T_c = \frac{9}{16\pi f_d} = 0.398\ ms.$$

For this coherence time, the necessary percentage of training symbols in the 2×2 system results in:

$$N_p = \frac{2T_s}{T_c} \times 100 = 33.51\%.$$

As a result, 1/3 of channel uses (33.33%) has been assigned to training symbols in all the evaluated range of $f_d T_s$ values (from $f_d T_s = 0.01$ to $f_d T_s = 0.03$), corresponding to a medium to high speed scenario. Following a similar analysis for the 4×4 system and, taking into account the increase of pilots in LTE (1.5 times more pilots in the 4×4 system than in the 2×2), 33.33% of training symbols is necessary for $f_d T_s = 0.02$. Nevertheless, we here show the results up to $f_d T_s = 0.03$ to be consistent with the represented values in the 2×2 case.

Note that, in the coherent schemes, data is transmitted within two blocks of length T carrying $3RT/2$ bits each to compensate the pilot overhead. To match the actual transmitted rate in bpcu, and hence be comparable with the non-coherent schemes, the constellations underlying the coherent codes have been carefully chosen as detailed in Table I.

B. Results

We evaluated the performance of the above mentioned schemes in terms of Frame Error Rate (FER) versus normalized Doppler frequency, i.e., $f_d T_s$, for T_s higher than 5σ, where σ stands for the channel delay spread [19]. A frame corresponds to 24 channel uses. This number was chosen as the minimum common multiplier of all the T values considered in this paper.

In Figure 5(a) and Figure 5(b), we compare the coherent and non-coherent schemes for $M = 2$ and a transmission rate of 2 and 3 bits per channel use, respectively. For $R = 2$ bpcu, a

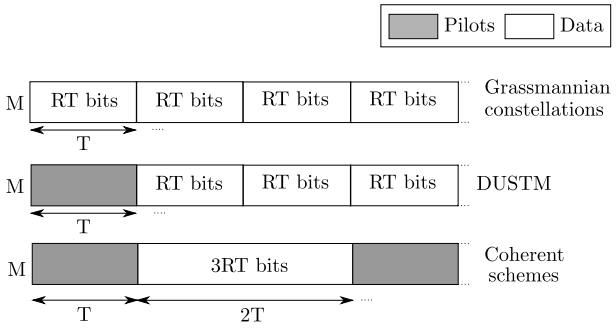

Fig. 4: Transmission configurations for the coherent and non-coherent schemes under evaluation.

TABLE I: Constellations selected for the coherent STBC schemes.

	Alamouti		**Golden**		**QOSTBC**	**3/4-STBC**
Rate (bpcu)	**2**	**3**	**2**	**3**	**2**	**2**
x-QAM	8	$2^{4.5}$	$2^{1.5}$	$2^{2.25}$	8	16

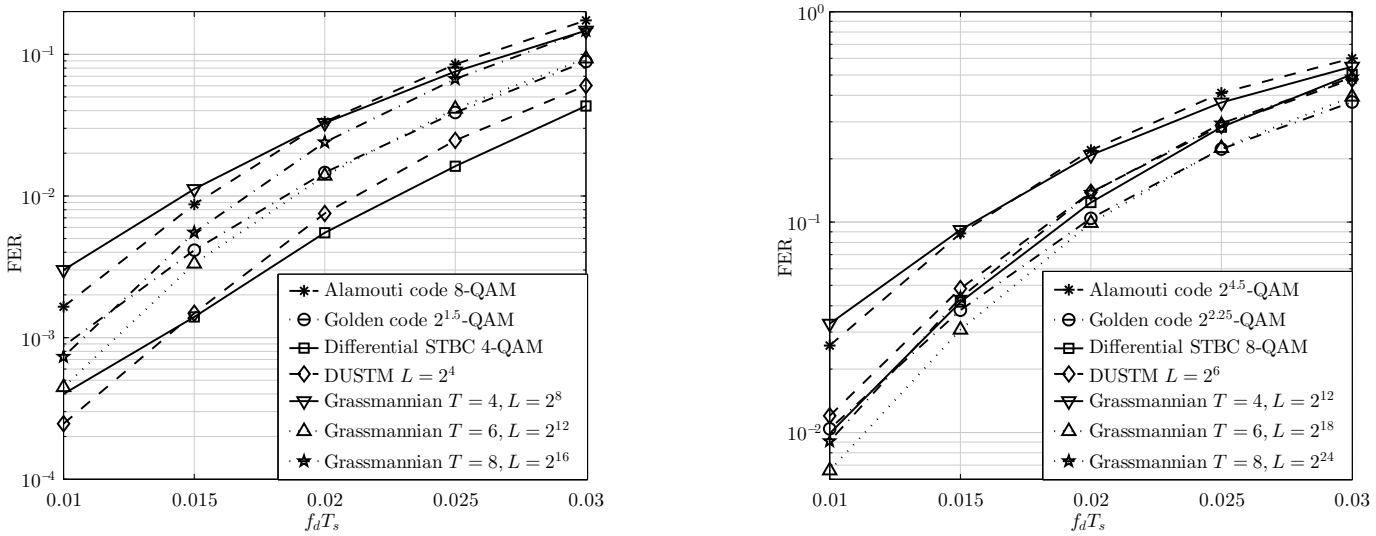

(a) $R = 2$. (b) $R = 3$.

Fig. 5: Performance comparison among coherent and non-coherent schemes with $M = 2$ assuming a temporally-correlated channel with different values of f_dT_s.

substantial performance degradation due to channel estimation errors is observed in the training-based schemes. Nevertheless, Alamouti coding outperforms Grassmannian signaling with $T = 4$ for f_dT_s values lower than 0.02. Beyond $f_dT_s = 0.025$, Grassmannian signaling has superior performance. Regarding the training-based Golden code, it outperforms Alamouti coding and two of the Grassmannian configurations ($T = 4$ and $T = 8$). It also matches the performance of Grassmannian signaling with $T = 6$ at high mobility. Concerning the differential schemes (DUSTM and differential STBC), both methods outperform the rest of schemes for all the evaluated values of f_dT_s. The differential STBC shows the best performance except for the lowest value, where DUSTM outperforms it. Overall, differential encoding looks like the best option for low data rates with medium to high mobility considered in this work. However, for $R = 3$, as shown Figure 5(b), the differential schemes exhibit poorer performance than the Golden code and Grassmannian schemes as the product f_dT_s increases. For medium mobility, non-coherent Grassmannian signaling is the best-performing scheme. However, note that, at high normalized Doppler frequency values, the Grassmannian signaling with $T = 6$ and the Golden code attain nearly the same FER values. Therefore, for the $R = 3$ case, non-coherent communication is only competitive at medium mobility, and based on Grassmannian signaling. Differential schemes should be discarded for $R > 2$ due to its performance degradation, which was already expected according to the results discussed in [3].

Focusing in the comparison among the different Grassmannian signaling configurations, it is important to note that increasing the length of the codewords is in general positive to increase capacity [2]. Indeed, this effect can be seen when comparing the $T = 4$ and $T = 6$ cases. However, Grassmannian constellations require the channel to be constant during the block and are, thus, sensitive to mobility and channel variability. For this reason, a block length of $T = 8$ offers worse performance than $T = 6$. This result suggests that an optimum block length can be found in temporally-correlated channels. Therefore, it can be concluded that in these channels, having a Grassmannian constellation with a longer block-length does not imply necessarily better performance, since the channel variations caused by mobility destroy the block-fading condition of the channel. This phenomenon is observed for both the $R = 2$ bpcu and $R = 3$ bpcu cases.

In Figure 6, we include the comparison between coherent and non-coherent schemes for $M = 4$ transmit antennas. We can see that non-coherent schemes perform much better than the coherent schemes for all the evaluated normalized Doppler frequency values. This motivates the interest in the design of new open-loop transmission techniques valid for higher-order MIMO configurations for vehicular communications. In fact, the rate-$3/4$ STBC suffers a higher performance loss than the rest of schemes. Unlike what is observed in Figure 5(a) for the 2×2 MIMO configuration with $R = 2$, the differential scheme (in this case only DUSTM has been evaluated) is no longer the best-performing scheme in a 4×4 MIMO system. Nevertheless, DUSTM still outperforms the coherent setups. The Grassmannian code with $T = 8$ outperforms all schemes with a significant advantage. As with the schemes with $M = 2$, increasing the Grassmannian block-length does not imply better performance. In fact, having a Grassmannian constellation designed for higher than $T = 8$ channel uses causes a performance loss due to mobility.

Note that, in the analysis of Figures 5 and 6, the relative speed between the transmitter and the receiver, the carrier frequency and the scenario under study are hidden through the normalized Doppler frequency. As an example of performance analysis as a function of the speed, we show in Table II the maximum speed where a maximum FER equal to 10^{-2} is satisfied, for the best analyzed coherent and non-coherent

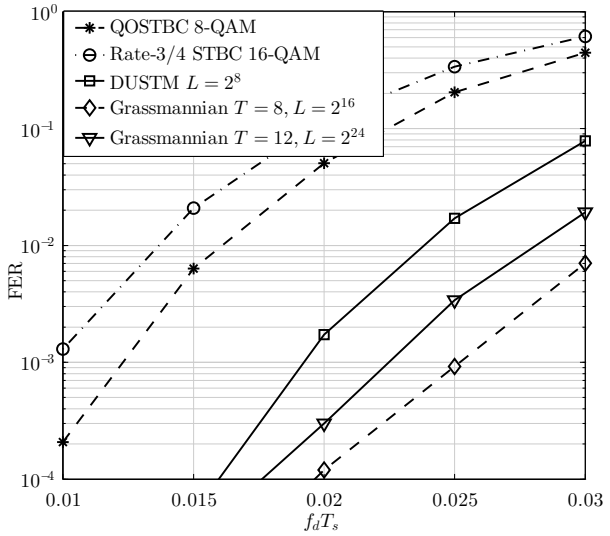

Fig. 6: Performance comparison among coherent and non-coherent schemes assuming a temporally-correlated channel with different values of f_dT_s for $R = 2$ and $M = 4$.

schemes. To this end, we considered the channel parameters described in the previous section. Table II shows that, while coherent and non-coherent schemes offer a similar maximum speed for two antennas, Grassmannian codes are a promising techniques for four antennas. In particular, the maximum supported speed by the non-coherent schemes almost doubles that of the coherent schemes, reaching up to 251 km/h in the latter case. This result motivates the interest in focusing on non-coherent schemes for vehicular communications, where a high number of antennas can be placed over a communicating vehicle and, also, where acquiring channel state information is a challenging task.

TABLE II: Maximum speed in km/h for the coherent and non-coherent schemes at FER$= 10^{-2}$.

	R=2		*R*=3
	M=2	*M*=4	*M*=2
Best coherent scheme	150	130	81
Best non-coherent scheme	184	251	92

VII. Conclusion

In this paper, a performance comparison between coherent and non-coherent signaling schemes under practical channel conditions has been carried out. In particular, the performance of these schemes has been evaluated over a temporally-correlated channel wherein the channel coefficients experience temporal correlation within each block. For two transmit antennas, we have compared the performance of DUSTM, differential STBC and Grassmannian codes with two coherent benchmark schemes based on Alamouti and Golden codes. For four transmit antennas, rate-3/4 and quasi-orthogonal STBC have been used for comparison.

At high SNR, our simulations show that, for a transmission rate of 2 bpcu and 2 transmit antennas, differential STBC offers the best performance from a given normalized Doppler frequency. For low normalized Doppler frequency, however, the DUSTM scheme slightly outperforms the differential STBC. Grassmannian signaling is otherwise unsuitable in this setup, since it is outperformed by coherent schemes at high mobility. When a higher transmission rate is considered, in particular 3 bpcu, differential STBC and DUSTM are outperformed by the coherent Golden code, due to their expected loss of performance for $R > 2$. Grassmannian signaling with $T = 6$ offers better performance than the rest of schemes for medium values of f_dT_s, although it shows a negligible performance gain with respect to Golden coding at high mobility. Therefore, non-coherent communication is not meaningful for $M = 2$, $R = 3$ and high mobility. For four antennas, there is a substantial performance advantage of non-coherent techniques against coherent ones, where the Grassmannian constellation of $T = 8$ outperforms all the rest. We show that this signaling is a very meaningful technique in scenarios with mobility and high SNR, especially for high number of transmit antennas, where the channel acquisition requires a high amount of pilot signals which penalize the data rate of coherent schemes. As a result, non-coherent communications and, in particular, Grassmannian signaling are promising techniques for vehicular communications with more than two transmit antennas with temporally-correlated channels affected by medium to high mobility.

Acknowledgement

The work of the UPV researchers was performed in the framework of the H2020 project METIS-II with reference 671680, which is partly funded by the European Union. The authors would like to acknowledge the contributions of their colleagues in METIS-II, although the views expressed are those of the authors and do not necessarily represent the project. The work of the Carleton researchers was supported in part by Huawei Canada Co., Ltd., and in part by the Ontario Ministry of Economic Development and Innovation's ORF-RE (Ontario Research Fund-Research Excellence) program

References

[1] J. K. Cavers, "An analysis of pilot symbol assisted modulation for Rayleigh fading channels [mobile radio]," *IEEE Trans. on Vehic. Tech.*, vol. 40, no. 4, pp. 686–693, Nov. 1991.

[2] L. Zheng and D. N. C. Tse, "Communication on the Grassmann manifold: a geometric approach to the non-coherent multiple-antenna channel," *IEEE Trans. Inf. Theory*, vol. 48, no. 2, pp. 359–383, Feb. 2002.

[3] B. Hochwald and W. Sweldens, "Differential unitary space-time modulation," *IEEE Trans. Commun.*, vol. 48, no. 12, pp. 2041–2052, Dec. 2000.

[4] V. Tarokh and H. Jafarkhani, "A differential detection scheme for transmit diversity," *IEEE J. Select. Areas Commun.*, vol. 18, no. 7, pp. 1169–1174, Jul. 2000.

[5] B. Hassibi and B. M. Hochwald, "Cayley differential unitary space-time codes," *IEEE Trans. Inf. Theory*, vol. 48, no. 6, pp. 1485–1503, Jun. 2002.

[6] R. H. Gohary and T. N. Davidson, "Non-coherent MIMO communication: Grassmannian constellations and efficient detection," *IEEE Trans. Inf. Theory*, vol. 55, no. 3, pp. 1176–1205, Mar. 2009.

[7] S. Roger, D. Calabuig, J. Cabrejas, and J. F. Monserrat, "Multi-user non-coherent detection for downlink MIMO communication," *IEEE Signal Processing Letters*, vol. 21, no. 10, pp. 1225–1229, Oct. 2014.

[8] Y. M. M. Fouad, R. H. Gohary, J. Cabrejas, H. Yanikomeroglu, D. Calabuig, S. Roger, and J. F. Monserrat, "Time-frequency Grassmannian signalling for MIMO multi-channel-frequency-flat systems," *IEEE Commun. Letters*, vol. 19, no. 3, pp. 475–478, March 2015.

[9] B. Le Saux, M. Helard, and P. Bouvet, "Comparison of coherent and non-coherent space time schemes for frequency selective fast-varying channels," in *2nd Inter. Symp. Wireless Commun. Systems*, Sienna, Italy, Sept 2005.

[10] S. Alamouti, "A simple transmit diversity technique for wireless communications," *IEEE J. Select. Areas Commun.*, vol. 16, no. 8, pp. 1451–1458, 1998.

[11] J. C. Belfiore, G. Rekaya, and E. Viterbo, "The Golden code: a 2x2 full-rate space-time code with nonvanishing determinants," *IEEE Trans. Inf. Theory*, vol. 51, no. 4, pp. 1432–1436, 2005.

[12] G. Ganesan and P. Stoica, "Space-time block codes: a maximum SNR approach," *IEEE Trans. Inf. Theory*, vol. 47, no. 4, pp. 1650–1656, May 2001.

[13] H. Jafarkhani, "A quasi-orthogonal space-time block code," *IEEE Trans. Commun.*, vol. 49, no. 1, 2001.

[14] Y. R. Zheng and C. Xiao, "Improved models for the generation of multiple uncorrelated Rayleigh fading waveforms," *IEEE Commun. Lett.*, vol. 6, no. 6, pp. 256–258, Jun. 2002.

[15] V. Tarokh, H. Jafarkhani, and A. R. Calderbank, "Space-time block codes from orthogonal designs," *IEEE Trans. Inf. Theory*, vol. 45, no. 5, pp. 1456–1467, Jul. 1999.

[16] B. Hassibi and B. M. Hochwald, "How much training is needed in multiple-antenna wireless links?" *IEEE Trans. Inf. Theory*, vol. 49, no. 2, pp. 951–963, Apr. 2003.

[17] C.-S. Hwang, S. H. Nam, J. Chung, and V. Tarokh, "Differential space time block codes using nonconstant modulus constellations," *IEEE Trans. Signal Processing*, vol. 51, no. 11, pp. 2955–2964, Nov. 2003.

[18] M. Beko, J. Xavier, and V. Barroso, "Non-coherent communication in multiple-antenna systems: Receiver design and codebook construction," *IEEE Trans. Signal Processing*, vol. 55, no. 12, pp. 5703–5715, Dec. 2007.

[19] T. S. Rappaport, *Wireless Communications: Principles and Practice*, 2nd ed. Prentice Hall, Jan. 2002.